interphase. This is in contrast with Kumar and Yoon,[6] where the average length of horizontal sequences seems to grow without bound. As the authors pointed out, this unphysical result may be due to their assumption of having a tight-fold energy without including an independent bending energy.

In Table V are listed the values of the order parameter for three values of c. Note that we observe again that the order parameter does not go to zero, but it tends to a negative value. As the tight-fold energy is increased, this effect is shown by the three approximations.

C. Conclusions. Our results have also been compared with Monte Carlo simulations.[2] We have found that there is no agreement when bending energy is larger than 0.8. We believe that this disagreement is due to the fact that the lattice used in the Monte Carlo simulations is not large enough to provide two independent interphases at the top and bottom of the lattice for high values of the bending energy.

From a comparison of the results obtained from our three approximations we found that the lattice model does not necessarily give better results with mathematical refinements. The second model is the simplest one and gives in most of the cases the most accurate results. We will therefore choose the second model in subsequent work where we study the effect of branches in the interface.

Acknowledgment. This research was supported by the National Science Foundation (Grant DMR-8706166), the donors of the Petroleum Research Fund, administered by the American Chemical Society, and by a NATO fellowship (I.Z.).

References and Notes

(1) Flory, P. J.; Yoon, D. Y.; Dill, K. A. *Macromolecules* **1984**, *17*, 862-868.
(2) Mansfield, M. L. *Macromolecules* **1983**, *16*, 914-920.
(3) Marqusee, J. A.; Dill, K. A. *Macromolecules* **1986**, *19*, 2420-2426.
(4) Helfand, E. *Macromolecules* **1976**, *9*, 307-310.
(5) Marqusee, J. A. *Macromolecules* **1989**, *22*, 472-476.
(6) Kumar, S. K.; Yoon, D. Y. *Macromolecules* **1989**, *22*, 3458-3465.
(7) Subroutine POWELL: Press, W. H.; Flannery, B. P.; Teukolsky, S. A.; Vetterling, W. T. *Numerical Recipes*; Cambridge University Press: Cambridge, U.K., 1986.
(8) Flory, P. J. *Principles of Polymer Chemistry*; Cornell University Press: Ithaca, NY, 1953; footnote on p 500 and p 504.
(9) Mathur, S. C.; Rodrigues, K.; Mattice, W. L. *Macromolecules* **1989**, *22*, 2781-2785.

γ-Isotactic Polypropylene. A Structure with Nonparallel Chain Axes

S. V. Meille,*,† S. Brückner,‡ and W. Porzio§

Dipartimento di Chimica del Politecnico di Milano, Piazza Leonardo da Vinci, 32, 20133 Milano, Italy, Istituto di Chimica della Università di Udine, Viale Ungheria, 43, 33100 Udine, Italy, and Istituto di Chimica delle Macromolecole del CNR, Via E. Bassini, 15, 20133 Milano, Italy

Received October 10, 1989; Revised Manuscript Received February 12, 1990

ABSTRACT: The crystal structure of the γ form of isotactic polypropylene (γ-iPP) is refined with the Rietveld method on X-ray diffraction data collected at low (-120 °C) temperature. The analysis, leading to the proposal of the totally novel crystal architecture with nonparallel chain axes, is discussed in detail, and the reliability of the proposed structure is assessed, also with reference to alternative models. While the overall structure is best represented in terms of the statistical copresence of anticlined isochiral helices at each crystallographic position, as implied by space group *Fddd*, local packing modes which cannot retain this feature are satisfactorily described in terms of space groups *F2dd* or *Fd2d*. Some relevant implications of the γ-isotactic polypropylene crystal structure on the crystalline morphology of this polymer are presented, while issues concerning the development of this novel architecture remain largely open to future contributions.

1. Introduction

The γ modification of crystalline isotactic polypropylene (γ-iPP) has attracted much attention over the years although interest in this polymorph for immediate applications has been modest, as it is obtained usually only in traces under normal crystallization conditions with commercial homopolymers. The appearance of the γ phase is favored by a molecular feature such as shortness of polymer chains[1] or, for long chains, by a physical variable such as high pressure.[2] An interesting paper by Turner-Jones describes also the influence that small amounts of comonomer units (4-10% ethylene or 1-butene) exert in promoting γ rather than α crystallinity in melt-crystallized copolymers,[3] which have indeed industrial importance.

High percentages of γ crystallinity are also obtained[4] with iPP synthesized with new homogeneous catalytic systems[5] for which future applications may be envisaged.

Crystallization in the γ phase has been related[6,7] to the reduced importance of chain folding, and investigations on the differences between the α and γ phases may contribute to clarification of this issue at a molecular level. A study on the relationships between chain folding and crystal structure was carried out for α-iPP, revealing the existence of a number of "selection rules" for neighboring

† Dipartimento di Chimica del Politecnico di Milano.
‡ Istituto di Chimica della Università di Udine.
§ Istituto di Chimica delle Macromolecole del CNR.

0024-9297/90/2223-4114$02.50/0

chains connected by tight chain folding.[8] These results raise the question of further verification on a possibly different structure. Another reason for studying the γ phase is that it seems to be involved in the process of homoepitaxial branching in the much more common α phase.[9] In fact, it is well-known that α-iPP presents a peculiar crystalline architecture where branching events, occurring with a well-defined geometrical relationship between daughter and mother lamellae, may be so frequent, under certain crystallization conditions, as to give rise to complex structures known as "quadrites".[10] Similar structures are also invoked to explain the anomalous positive birefringence in α-iPP spherulites.[11]

Other experimental observations on γ-iPP revealed contradictory aspects about this structure. On the one hand, it shows a powder X-ray diffraction profile that bears great resemblance to that of α-iPP, thus suggesting the possibility that only a modest distortion of the crystal lattice parameters is sufficient to account for the transition from the α to the γ structure.[1] On the other hand, the crystal morphology of γ-iPP presents a distinct lamellar shape, a different lattice orientation with respect to the long lamellar direction, and a highly unusual chain axis tilt relative to the lamellar surface.[7] We also recall that the hypothesis of a simple relation between the α and γ structures, in terms of some distortion of lattice parameters, has been ruled out by packing calculations that never revealed the existence of a secondary minimum in the neighborhood of the α structure.[12]

The marked differences existing between the γ and the α phases of iPP are finally well illustrated by the intrinsic instability of γ-iPP upon stretching of the sample,[13] an operation that leads to the α modification. Obviously enough, this prevents any analysis based on the usual fiber diffraction approach.

The interest for a detailed knowledge of the structural features of γ-iPP and the availability of a computer program, written by Immirzi[14] and improved by one of the authors to deal specifically with polymer structures,[15] which allows for crystal structure refinements based on the Rietveld method,[16] prompted us to undertake the task of determining and refining the molecular structure of γ-iPP starting from powder X-ray diffraction data.

In a preliminary communication[17] we reported on the essential features of the crystal structure of γ-iPP. The architecture we find is totally new for a macromolecular system; we can summarize it as a layer structure where nonparallel chain axes coexist, the change of direction occurring between adjacent layers. The fundamental step in the γ-iPP structure determination was the recognition that the triclinic cell (a = 6.54 Å, b = 21.40 Å, c = 6.50 Å, α = 89°, β = 99.6°, γ = 99°, cell I) proposed by Morrow and Newman[1] is in disagreement with a number of experimental data,[17] which led us to the determination of a revised triclinic cell (a = 6.55 Å, b = 21.57 Å, c = 6.55 Å, α = 97.4°, β = 98.8°, γ = 97.4°, cell II). These new lattice parameters, giving rise to a complete and satisfactory indexing of all observed reflections, also meet the stringent requirements that allow or better impose the transformation to a face-centred orthorhombic cell (a = 8.54 Å, b = 9.93 Å, c = 42.41 Å, cell III).

We want to emphasize that the most unusual features of the architecture we find are already envisageable in the symmetry of cell III, *prior to any detailed definition of the structural model*, the only assumption being that iPP crystallizes in the usual TG conformation giving rise to the well-known 3_1 helix with a periodicity of 6.5 Å. This length is one-half of the diagonal of the (a,b) plane in cell III, and the only possibility for an object, with the given periodicity, to be located in cell III is to be parallel to one of the diagonals of the (a,b) plane. Symmetry however requires a second chain to be parallel to the other diagonal, with the consequence of imposing the coexistence of nonparallel chain axes within the same crystal lattice.

Table I
Experimental Conditions of Data Recording

instrument	Siemens D-500 goniometer equipped with step–scan attachment, proportional counter, and Soller slits, controlled with an Olivetti M24 computer
radiation (power)	Cu Kα, Ni-filtered (40 kV, 30 mA)
divergence aperture, deg	0.3
receiving aperture, deg	0.05
step width, deg	0.03 (2θ)
count time (seconds per step)	50
2θ range, deg	10–60
temp, °C	−120

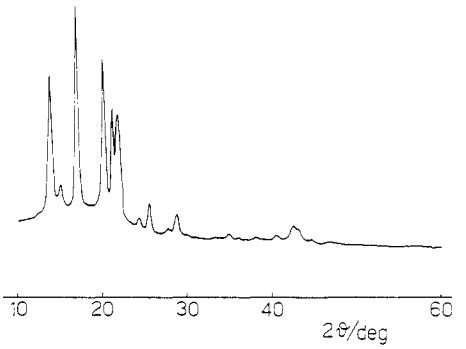

Figure 1. Experimental X-ray diffraction profile of γ-iPP recorded at −120 °C.

In this paper we describe in detail the procedure followed to solve the γ-iPP crystal structure and the results obtained by refining the structural model on powder X-ray diffraction data collected at low temperature (−120 °C). The data leading to what we believe to be the univocal determination of the unit cell and space group are discussed together with the reliability of the refined model. Finally, we present some considerations on the local rather than the statistical packing and on the consequences that the knowledge of this structure involves in explaining, at a molecular level, some of the mentioned peculiarities of crystalline iPP.

2. Experimental Section

Isotactic polypropylene, synthesized by using the homogeneous catalyst methylalumoxane–*rac*-ethylenebis(4,5,6,7-tetrahydro-1-indenyl)dichlorozirconium,[5] was supplied by L. Resconi of Himont, Novara. The preparation and the GPC and NMR characterization are fully given in ref 18, sample E. Crystallization conditions are described in ref 17.

Powder diffraction data were obtained according to the conditions given in Table I. A temperature control device (Model TTK developed by Anton and Parr) was attached to a computer-controlled Siemens D-500 instrument. The sample was kept under vacuum (10^{-2} mmHg) at −120 ± 0.4 °C with a slow flux of liquid nitrogen.

3. Results

In Figure 1 we report the powder X-ray diffraction profile of γ-iPP collected at −120 °C, while further details on the experimental conditions of data collection are given in Table I. The profile in Figure 1 is qualitatively similar

to the one collected at room temperature,[17] but a more accurate analysis shows a better signal-to-noise ratio, particularly at high 2θ values, and an enhanced contribution of the crystalline part relative to the amorphous component. Small changes in peak positioning are in agreement with a contraction of the unit cell, which is now $a = 8.51$, $b = 9.95$, $c = 41.68$ Å. Note that while a and b and consequently the (a,b) plane diagonals corresponding to twice the chain axis repetition are constant within experimental error, the c axis is reduced by ca. 2% with respect to its room temperature value.

The structural analysis was carried out in the *Fddd* space group symmetry in view of the better agreement with the observed data. This symmetry requires a 50% statistical substitution of anticlined chains at the same crystal sites in analogy with the situation encountered by Natta and Corradini in α-iPP (space group $C2/c$).[19]

Alternatively, two additional space groups were also tested, i.e., *Fd2d* and *F2dd*. The substantial difference from *Fddd* is that these groups do not require any statistical superposition of anticlined chains. They are expected therefore to give a better representation of the real *local* situation in the crystal under the reasonable assumption that the 50% substitution results as an overall effect due to the contribution of a number of crystal domains where more selected arrangements occur. This situation again shows an analogy with that found in α-iPP where space group $P2_1/c$ is adopted when departures from equiprobable anticlined substitution are determined:[20] indeed energy calculations[12] show $P2_1/c$ packing to be favored, and this symmetry is generally thought to dominate locally in α crystals.[8]

Only one threefold helical unit (three monomers) is sufficient to generate the whole γ-iPP crystal structure. As already stated, chain axes must be located parallel to the (a,b) plane diagonal, which measures twice the helical repeat, i.e., 13.09 Å. In space group *Fddd* the need for locating methyl groups belonging to superimposed anticlined chains approximately at the same positions in the crystal requires the chain axis to intersect the twofold axes parallel to c and constrains one methyl to lie very close to the same twofold axes. The only remaining degree of freedom is the translation along the c direction. However, the very strong intensity of the 008 reflection requires that layers of chains orthogonal to c be spaced approximately by $c/8$, and in order to achieve this, the z coordinate of the molecular axis must be very close to $\pm 1/16$. A detailed examination of space group *Fddd* shows that only two distinct families of models with encouraging packing and meeting all the above requirements must be examined. The two models (see Figure 2 and its caption) show some common features: (i) Both consist of layers of parallel isochiral helices perpendicular to the c axis of the γ-iPP crystal structure. (ii) Each of these layers is related by a glide plane operator (and also by a center of symmetry in *Fddd*) to one contiguous layer, which therefore consists of helices parallel to those in the reference layer but of opposite chirality. Two such adjacent parallel layers form what we will call a bilayer. (iii) Each layer gives rise (through twofold axes parallel to a and/or b) to a contiguous layer of helices with the same chirality of the reference layer and rotated around the c axis by ca. +81° or −81°, depending upon the chirality of the helices. (iv) The packing within bilayers of the two models (see Figure 2) closely corresponds to the modes of packing of planes perpendicular to the b direction (long axis) in the α-iPP crystal structure.[19] (v) Similarly, the distinct mutual arrangements of contiguous bilayers in the two models

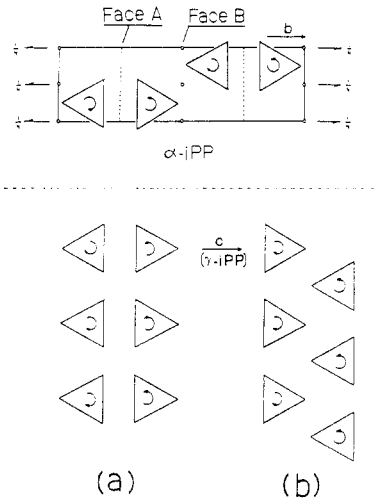

Figure 2. Schematic view of the c-axis projection of the α-iPP unit cell (space group $P2_1/c$. Following ref 21, the two distinct, possibly exposed, $0k0$ faces are evidenced respectively as face A and face B. Correspondingly, the two different bilayers a and b, orthogonal to the long crystallographic axis b, which can be identified in the α-iPP crystal structure, are shown. Bilayers consist of two individual layers; within each layer helices are homochiral but the two contiguous layers making up both bilayers are composed of helices of opposite chirality. Both a and b are conceivable starting arrangements for parallel-chain bilayers in the γ-iPP crystal structure, as they are compatible with the *Fddd* space group and pack reasonably. In this structure bilayers are orthogonal to the c axis (cell III). Arrangements a and b are referred to respectively as models I and II in the text. It is important to note that a-type parallel-chain bilayers (model I) require that in γ-iPP the 80° tilting occurs at face B, whereas tilted type b bilayers (Model II) would pack along face A.

reproduces the two packings suggested as schemes to account for α–α branching at a molecular basis.[11,21] Although both starting models present feasible packing, the powder diffraction data are highly discriminative and structural refinement, at first carried out in the rigid-body approximation, yields dramatically different results. At this initial stage the disagreement factor R_2', calculated as $\sum|I_o - I_c|/\sum I_{net}$, where $I_{net} = I_o - I_{backgr}$ and I_{backgr} includes the amorphous contribution, equals respectively 0.16 for model I and 0.60 for model II.

Subsequent refinement was accordingly performed only on model I, allowing for small deviations from the ideal TG conformation while keeping a rigorous 3_1 symmetry. This was done by adopting the same approach followed by Immirzi in the study of α-iPP;[14] i.e., two adjustable parameters, τ and ϕ, were allowed to deviate from their ideal values of 1.0 and 120° in order to give a better fitting with the observed data.

Nonstructural parameters were refined as well; in particular, the background contribution was evaluated in the form of a segmented line whose nodes could be refined on the intensity scale. The peak shape was assumed to be a Cauchy function with half height width depending on the given hkl values through an adjustable estimation of the average crystallite dimensions.[22,23] A zero-point correction on the experimental 2θ scale was evaluated and a (small) preferred orientation effect detected.

The final disagreement factor R_2' was 0.114 while the conventional R_{wp} factor was 0.055. Note that the value of R_2' is substantially better than the figures obtained for ambient temperature Rietveld refinements of both α-iPP[14] ($R_2' = 0.154$) and γ-iPP[17] ($R_2' = 0.152$). From the crystallographic point of view it is worthwhile to point out that in the powder profile no substantial peak overlap occurs up to $2\theta = 27°$. This is a particularly favorable

Table II
Refined Nonstructural Parameters

zero correction (2θ), deg	−0.042 (5)
preferred orientation[a]	G = 0.110 (6); indices 001
profile function parameters[b]	
U	2.03 (4)
V	−0.54 (3)
W	different for each reflection (see text)
m	1
intensities (k counts) at the points on the segmented line	
10° 2θ	0.705 (9)
16° 2θ	0.775 (6)
23° 2θ	0.567 (5)
30° 2θ	0.366 (3)
40° 2θ	0.283 (2)
60° 2θ	0.139 (2)

[a] Preferred orientation factor PO = $\exp(-G\alpha_k)$, where α_k is the angle between the scattering vector of the kth reflection and the scattering vector of a fixed (preferred) reflection. [b] Peak shapes are calculated analytically through a Pearson VII function: $f(z) = (C/H_k)[1 + 4(2^{1/m} - 1)z^2]^{-m}$, with $z = (2\theta_i - 2\theta_k)/H_k$ and $H_k^2 = U\tan^2\theta_k + V\tan\theta_k + W$; $m = 1$ determines a peak profile following a Cauchy distribution.

Table III
Refined Fractional Coordinates of the Asymmetric Unit[a]

	x	y	z
C(1)	−0.1443	−0.0871	0.0450
C(2)	−0.1080	−0.0278	0.0781
C(3)	−0.2608	0.0179	0.0944
C(4)	0.0144	0.0854	0.0794
C(5)	0.1776	0.0519	0.0659
C(6)	0.2493	−0.0665	0.0844
C(7)	0.2962	0.1679	0.0640
C(8)	0.2454	0.2909	0.0444
C(9)	0.2120	0.2493	0.0096

[a] Isotropic thermal factors for non-hydrogen atoms are B = 1.5 Å^2. The values of τ and ϕ[14] are 114.5 and 1.01°, respectively.

situation for Rietveld analysis since peak overlapping is the most severe weakness of powder diffraction approaches in comparison with the traditional fiber diffraction analysis. The agreement we observe with experimental data is therefore even more significant than in normal cases.

In Table II the refined nonstructural parameters are listed, while in Table III we report the fractional coordinates of the carbon atoms belonging to the independent structural unit together with parameters τ and ϕ. In Figure 3 we show a comparison between the observed (curve a) and the calculated (curve b) profiles, whereas curve c is the difference profile.

As already stated *F*2*dd* and *F*d2*d* space groups were taken into account as well. Both of them suppress the twofold axis parallel to *c* but they differ in locating a twofold axis parallel to *a* (*F*2*dd*) or to *b* (*Fd*2*d*). Refinement in *F*2*dd* and *Fd*2*d* symmetry gave a disagreement factor R_2' of 0.130 and 0.141, respectively.

4. Discussion

In polymer science fiber diffraction is the technique of choice to determine macromolecular crystal structures, while other experimental procedures such as powder diffraction or single-crystal electron diffraction are used less frequently. There are, however, instances, such as the one discussed in the present paper, in which the fiber diffraction approach cannot be used because orientation has disturbing influences on the crystalline phase to be examined or else macroscopic oriented samples cannot be obtained. Under the circumstances we feel that the issue

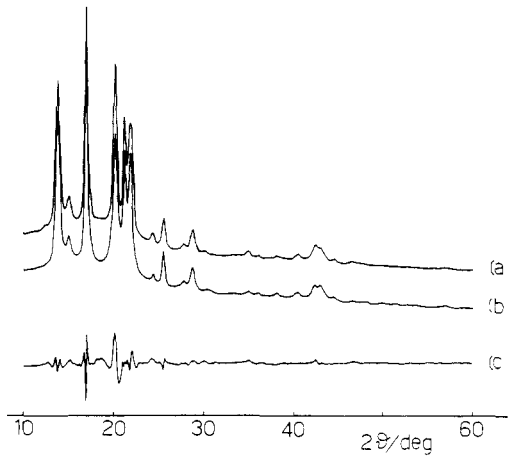

Figure 3. Comparison of the observed (curve a) and the calculated (curve b) powder diffraction profiles of γ-iPP. Curve c is the difference profile.

of how the reliability of crystal structures obtained by Rietveld analysis compares with traditional approaches should be addressed openly.

Structure determination by powder profile analysis is becoming increasingly common. The number of structures refined with this technique has grown from a few hundred in the early eighties to currently well over one thousand. Among the available reviews, the work by Albinati and Willis[24] appears particularly pertinent to our discussion. These authors, comparing single-crystal and powder refinements, conclude that "in spite of theoretical limitations .... the Rietveld method appears to give reliable values for the structural parameters and reasonable values of the correspondent standard deviations". They also note that while the powder method does not usually allow for determination of the space group or for solution of the phase problem, *except for very simple structures*, "the important contribution of Rietveld was to recognize that structures could be refined from powder data even where there was severe overlapping of diffraction peaks. The essential idea was to forget about individual Bragg reflection and refine the pattern as a whole."

Research in our laboratories[15,25-30] and from other groups[31-33] demonstrates that similar considerations apply also to the analysis of polymer crystal structures. It has been indeed clearly shown[14,29,30] that the results of Rietveld refinements are closely comparable to reliable fiber analysis and discriminative with respect to approximate models in cases where such data were available. Our experience suggests that in the analysis of polymer crystal structures using powder X-ray diffraction profiles, the following simple guidelines are useful:

(1) Obviously enough, all the observed diffraction maxima in the powder spectrum should be consistently indexed.

(2) The proposed model should be in close agreement with all reliable data available from other techniques: (i) the chain repeat (from pertinent fiber analysis and/or conformational calculations); (ii) the unit cell and space group obtained from critically evaluated electron diffraction data.

(3) The solution of the structure in cases where the molecular conformation is basically known should be attempted by rigid-body analysis. Refinement of a solved structure should be constrained, i.e., performed allowing only for torsion and minor bond angle adjustments.

(4) In polymer crystal structure analysis it is necessary to empirically correct for scattering due to the amorphous component; thus a meaningful measure of the quality of

the model is given by $R_2' = \sum|I_o - I_c|/\sum I_{net}$, where $I_{net} = I_o - I_{backgr}$ and I_{backgr} includes the amorphous contribution, which can be modeled in different ways.[14,33] R_2' measures accordingly the agreement over the crystalline component, whereas $R_{wp} = [\sum w(I_o - I_c)^2/\sum I_o^2]^{1/2}$ is artificially lowered as I_o includes also the contribution of the amorphous profile. Indeed even with high amorphous content R_2' remains significantly different for different structural models, while R_{wp} becomes increasingly insensitive. Typical values of R_2' for correctly solved polymer structures range between 0.10 and 0.20,[14,15] while for R_{wp} values of 0.10 or lower are usually obtained. It is furthermore important that the disagreement level be roughly uniform over the whole diffraction profile: in fact, in the refinement of a single crystalline phase, obtaining a reasonable overall fit while even a single prominent peak of the powder profile is not reproduced strongly suggests unreliability of the model. Note that whereas the calculated values of the structure factors are comparable to those obtained by any X-ray diffraction structure analysis, preferred orientation effects, peak overlapping, and the amorphous contribution affect observed intensity data, preventing simple meaningful comparisons with other experimental data.

(5) Packing tests checking for unfavorable intermolecular contacts are useful to discriminate among possible starting models, while being obviously mandatory for the final structure.

Let us now examine, following the above guideline, the reliability of the proposed γ-iPP crystal structure. The discussion will initially be centered on the revised primitive unit cell (a = 6.55 Å, b = 21.57 Å, c = 6.55 Å, α = 97.4°, β = 98.8°, γ = 97.4°, cell II). Contrary to the previously proposed unit cell (a = 6.54 Å, b = 21.40 Å, c = 6.50 Å, α = 89°, β = 99.6°, γ = 99°, cell I),[1] cell II accounts for the diffraction maximum at 2θ = 24.5° (−120 °C), already identified in the work of Turner-Jones et al.[13] With cell I no diffraction maxima are calculated in the 23.7–25.1° 2θ range. Electron diffraction data pertaining to the $hk0$ projection have been published by different authors,[1,7] while the geometric concordance of the γ-iPP $h0l$ reciprocal lattice projection with the α-iPP $h0l$ projection, implied by the α–γ branching mechanism, has been discussed by Lotz et al.[7] Indeed the mentioned reciprocal lattice projections define the reciprocal lattice parameters a^*, b^*, c^*, β^*, and γ^*, which in the two examined unit cells are in very close agreement. Additional and conclusive evidence is obtained from the single-crystal electron diffraction pattern published in ref 7, Figure 5. Just three pairs of reflections can be identified in this pattern: the first is the 040 reflection defining the b^*-axis orientation; one of the other two pairs, both with d = 4.19 Å (room temperature), can be indexed with both unit cells as reflection 101, while the third pair must have the same h and l values of the second but differ not by one k unit, as suggested by the authors of ref 7, but by two k units. No reflection complying with the above requirements is calculated with cell I, whereas cell II allows indexing of the above reflection as $1\bar{2}1$. The alternative indexing of the third reflection as 121 yields an untenable unit cell as the strong reflection with d = 4.05 Å (see Table IV) is unindexed. At this point the correctness of cell II (which is a primitive negative reduced cell, and thus unique[34]) should be considered established, as it is able to account for both the observed powder patterns and electron diffraction data, while on the contrary cell I displays disagreements with both data sets.

The lattice parameters of cell II permit the transformation to the face-centered orthorhombic cell III which just represents a geometrical construction allowing for full exploitation of the symmetry operators implied by the lattice. The requirements for such a transformation are very stringent: the identity of a and c and of α and γ are indeed necessary but not sufficient as a third complex relationship[34] ($\mathbf{a}\cdot\mathbf{c} = -(\mathbf{a}\cdot\mathbf{a} - 2|\mathbf{b}\cdot\mathbf{c}|)$) is required. It certainly appears extremely unlikely that all three relationships can be satisfied as a result of mere chance. Indeed the face-centered orthorhombic lattice agrees also with the pattern of lattice parameter contraction on going from ambient temperature to −120 °C (vide supra). Furthermore, although the fact is never acknowledged, possibly because it would require a unit cell axis of over 40 Å, published electron diffraction patterns appear to be generally consistent with the above result. Specifically, patterns obtained from single crystals such as the one already discussed, reported in ref 7, Figure 5 (hkl reciprocal lattice projection with cell II indexing), and $hk0$ patterns (cell II indexing) reported in ref 1, Figures 6a,b and 8a,b, are suggestive of an orthorhombic lattice. The $hk0$ diffraction patterns obtained from an α-iPP lamella with branching γ crystals discussed in ref 7, Figure 2, clearly display the same symmetry. However, this feature is explained by the authors stating that "for the γ overgrowths the whole α-phase lamella acts as a plane of symmetry" and that "this relationship must be associated with the existence of a corresponding symmetry at a molecular level in the α-phase mother lamella". In other words, the helices exposed on the opposite 010 faces of the α lamella are supposed to be consistently of opposite chirality and to nucleate enantiomorphic γ-iPP crystals. Hence the orthorhombic symmetry is thought to be due to superimposition of the images of the enantiomorpic triclinic lattices on which the α lamella acts as a plane of symmetry.

The evidence supporting this model consists of two selected-area diffraction patterns taken from opposite sides of an α lath with γ overgrowths (Figure 3, ref 7). Examination of the corresponding original patterns, kindly provided by the authors, indicates that the deviations from the orthorhombic symmetry involve the reflection intensity and not their geometry. In any case, puzzling features are apparent:

Table IV
Comparison between Cell III and Cell II Indexing for γ-iPP[a]

cell III hkl	2θ,[b] deg	d, Å	$\lvert F_c\rvert$	cell II hkl
111	13.86	6.39	29.3	100, 001, $1\bar{1}0$, $0\bar{1}1$
113	15.11	5.86	12.3	110, 011, $1\bar{2}0$, $0\bar{2}1$
008	17.02	5.21	54.6	040
115	17.36	5.11	12.9	120, 021, $1\bar{3}0$, $0\bar{3}1$
022	18.33	4.84	3.0	$\bar{1}11$, $11\bar{1}$
117	20.27	4.38	37.3	130, 031, $1\bar{4}0$, $0\bar{4}1$
202	21.32	4.17	40.1	$1\bar{2}1$, 101, 050
026	21.97	4.04	51.3	$\bar{1}31$, $13\bar{1}$
119	23.63	3.76	1.7	140, 041, $1\bar{5}0$, $0\bar{5}1$
206	24.54	3.63	12.1	$1\bar{4}1$, 121
0,0,12	25.65	3.47	34.2	060
1,1,11	27.28	3.27	5.7	150, 051, $1\bar{6}0$, $0\bar{6}1$
220	27.58	3.23	3.2	$2\bar{1}0$, $0\bar{1}2$
222	27.92	3.20	8.7	200, 002, $2\bar{2}0$, $0\bar{2}2$
0,2,10	27.92	3.20	9.7	$\bar{1}51$, $15\bar{1}$
224	28.91	3.09	22.0	210, 012, $2\bar{3}0$, $0\bar{3}2$
131	28.94	3.08	9.3	$\bar{2}11$, $\bar{2}01$, $\bar{1}02$, $11\bar{2}$
133	29.61	3.02	1.0	$\bar{2}21$, $\bar{1}12$, $21\bar{1}$, $12\bar{2}$
2,0,10	30.02	2.97	2.4	$1\bar{2}1$, 101, 070

[a] All the space group allowed reflections in the 10–30° 2θ range are shown (2θ and d values at −120 °C). Absolute values of calculated structure factors for the final model in cell III (face-centered orthorhombic) are also listed. [b] Cu Kα.

(1) In one pattern, where the γ-phase contribution is more asymmetric, also reflections that should be symmetric (e.g., γ 040, cell II indexing) display markedly different intensities.

(2) In the second pattern, more symmetric with respect to the γ-phase contribution, a clear undue asymmetry is also detected among the intensities of equivalent $hk0$ reflections of the α phase.

The interpretation of the above results is not straightforward, and some specimen tilting could be suggested as the possible source of unexpected asymmetries. In any case we think that attempts of solution of the γ-iPP crystal structure assuming true triclinic symmetry, in accordance with previous hypotheses, and utilizing the revised unit cell II, should be briefly discussed. This, of course, amounts to considering the relationship among lattice parameters in cell II only approximate, and in any case accidental, and allows for parallel-chain models. Both the $P\bar{1}$ and the $P1$ space groups, with respectively two and four threefold helical segments in the asymmetric unit, were considered, testing a large number of starting models obtained either as perturbations of the α-crystal structure or completely independently. Rigid-body analysis was attempted initially while adjustments of the intramolecular conformation were allowed on the comparatively better attempts. As already mentioned in a previous note,[17] the 18–25° 2θ region could never be adequately reproduced. The typical values of the disagreement factors R_2' and R_{wp} were respectively ca. 0.22 and 0.13 for the best models. It is interesting to note that they compare well with those recently reported[35] for other attempts of parallel-chain refinement of the γ-crystal structure using both cell I and a different unit cell (a = 6.60 Å, b = 10.65 Å, c = 6.80 Å, α = 89.3°, β = 102.2°, γ = 99.3°), related to the original Turner-Jones cell,[13] but with the chain repeat axis increased by ca. 5%. The fact that for different models similar disagreement factors are obtained, however, substantially (two- to threefold) higher than those reported for correctly solved polymer structures (vide supra), indicates that none of the attempted parallel-chain solutions of the γ-iPP crystal structure can be correct. This conclusion is additionally supported by the fact that the mismatch between observed and calculated spectra is mainly concentrated in a limited angular region and by the disagreement of the assumed unit cells with clear experimental evidence. The results of the successful refinement using the orthorhombic cell III and space groups *Fddd*, *F2dd*, and *Fd2d* have been presented in the previous section. At this stage it appears worthwhile to mention that the disagreement factors for both the ambient temperature data (R_2' = 0.152, R_{wp} = 0.058) and the low-temperature refinement (R_2' = 0.114, R_{wp} = 0.055) are comparable to or better than for Rietveld refinements reported for the correct crystal structures of other polymers. The fit is also dramatically better than the one obtained for any γ-iPP refinement with truly triclinic cells keeping the chain axes parallel. The observed agreement is even more significant if we note that the degrees of freedom using the face-centered orthorhombic cell are substantially less than with the triclinic cell:

(1) Three refinable lattice parameters are needed to index all the observed reflections against six in the triclinic case.

(2) Practically all observed powder diffraction maxima up to 2θ = 27° are uniquely indexed with the orthorhombic cell, while severe multiple peak overlapping occurs with cell II or cell I (see Table IV). Indeed the larger volume of cell III does not involve a higher density of peaks on the 2θ axis since the systematic absences resulting from the face-centered symmetry keep the number of allowed diffraction maxima smaller than that predicted with primitive cells I or II.

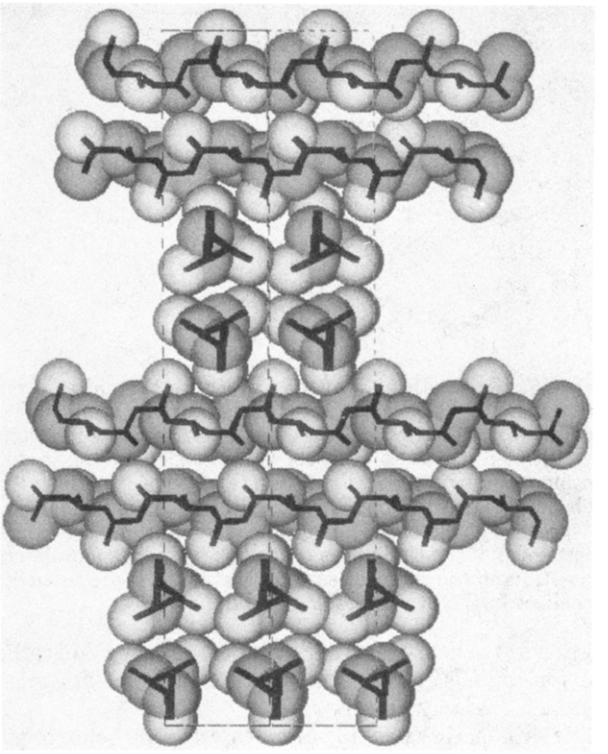

Figure 4. Packing diagram of γ-iPP drawn with SMILE:[39] the view axis coincides with one of the two helix axis orientations in the crystal, i.e., with one of the (a,b) plane diagonals. Coaxial anticlined helices are omitted for clarity. Note the favorable interdigitation of methyls.

(3) The asymmetric unit is only one threefold helical unit in space group *Fddd*, while two or four units are respectively necessary in space groups $P\bar{1}$ and $P1$.

The analysis of packing interactions yields additional confirmation of the correctness of the structure we propose. Figure 4 shows the crystal packing viewed along one diagonal of the (a,b) plane. Statistically superimposed chains are omitted for the sake of clarity.

As already stated, *Fddd* symmetry arises as an average situation reflecting the statistical arrangement of anticlinic and cataclinic chains in a large assembly. An analysis of packing contacts is therefore expected to result in an "excess" of data, some of them being unrealistic, depending on whether that particular contact is actually present in the crystal or not. This is particularly true for contacts involving methyl groups, which play a determinant role in stabilizing intermolecular arrangements. Inspection of Figure 4 immediately reveals a substantially favorable interdigitation of methyl groups, and this is confirmed by the calculation of packing distances on the model resulting from refinement against X-ray data. The shortest methyl–methyl contacts lie in the 3.7–4.0-Å range, the lower extreme being somewhat shorter than expected, thus indicating that a pure random substitution of chains with opposite direction is a simplified model and a more precisely defined correlation between neighboring chains may exist. This possibility is also supported by packing calculations carried out in the *F2dd* and *Fd2d* symmetries. While in space group *Fd2d* the more unfavorable contacts are maintained, in *F2dd* the shortest methyl–methyl contacts disappear (the closest one is at 4.0 Å) with an overall improvement in the steric situation. This fact,

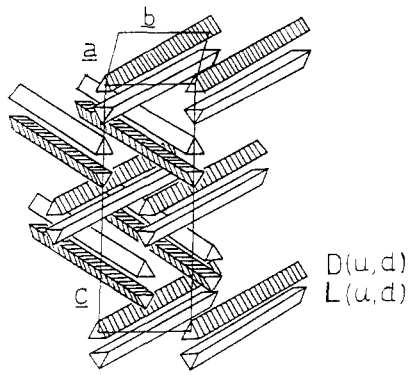

Figure 5. Schematic view of the γ-iPP crystal architecture. D (striped) and L (clear) labels refer to the chirality of the helices, while the (u,d) subscript indicates that helices of opposite polarity (i.e. anticlined) are statistically copresent at each crystallographic position. Chains run parallel to the (*a*,*b*) plane diagonals, and layers parallel to the (*a*,*b*) plane, consisting of homochiral helices, are apparent. The chirality of helices in adjacent layers is of opposite sign if the chain axes in the two layers are parallel. On the contrary, if the chain axes in contiguous layers are tilted 80°, the helices in the two layers are isochiral.

together with the better R_2' factor obtained for *F*2*dd* rather than for *Fd*2*d*, is an indication that the local packing might approach *F*2*dd* symmetry.

The satisfactory packing of methyl groups belonging to adjacent layers of chains *of the same chirality* and tilted with respect to each other at 80° has already been recognized by some authors[11,21] on the basis of molecular modeling aimed at interpreting the peculiar phenomenon of branching in α-iPP. This is an example of the fact that the overall architecture of γ-iPP, while certainly representing a novelty in the field of crystalline polymers, contains, at the same time, a number of local features that are not unexpected. In fact, they have already been considered for possible explanations of the complex behavior of crystalline iPP. However, of the two packings suggested to account for the 80° chain axis tilting in α–γ branching, only one (see Figure 2a) actually occurs, while the other (Figure 2b), although compatible with the space group symmetry and with roughly acceptable packing, is ruled out by the diffraction profile of the γ phase.

In Figure 5 we show a schematic representation of the γ-crystal architecture we determined. It may be seen that, along *c*, there is a regular repetition of the crossing event that, isolated, is expected to occur at the interface between branching α-phase lamellae.

We may finally observe that the laws that govern the growth of the α phase and of the γ phase are different, but in both cases the deposition of a new chain on the 010 face in the case of α-iPP and on the 001 face (cell III indexing) for the γ modification is univocally determined by the nature of the crystal surface. If, adopting the convention of ref 21, we label with A and B the two types of surfaces encountered along the *c* direction (cell III) in the γ modification (Figure 2), the rule driving the crystal growth along the corresponding direction can be summarized as follows: a substrate of type A *always* (both in α-iPP and in γ-iPP) induces deposition of chains of opposite chirality and parallel to the substrate chains, while an exposed face of type B in the γ modification always induces deposition of chains of the same chirality but tilted with respect to the substrate chains, the tilt angle being ±81° according to the chirality of the chains. The obscure point appears to be the reason for which substrates of type B in the α and in the γ phases induce a different pattern of deposition. In this respect we want to point

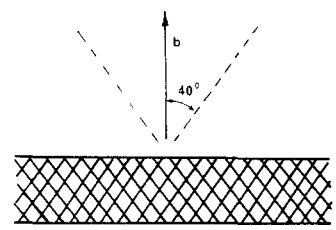

Figure 6. Sketch of a γ-iPP crystal seen in sideways projection. The horizontal lines define the lamellar surfaces. The two chain axis orientations defined by the striped pattern form a 40° angle with the normal to the lamellar surface.

out that we are dealing with a probably unique situation. In fact, iPP meets the very peculiar condition of having the chain-repeat period equal to a crystallographic interchain distance. This is well-known but it means also that the "decision" of a chain to crystallize parallel or tilted relative to the chains in the crystalline substrate may be influenced by subtle effects. The substantial equivalence of the two arrangements from the point of view of intermolecular contacts is testified by the packing analysis of the present model and will be further confirmed by the results of the energy calculations which are being completed.[36] If we accept this point the consequence is that nothing bizarre happens in the case of γ-iPP with respect to α-iPP: indeed in both cases the condition that the deposition of a new chain be univocally determined by the nature of the crystal surface is satisfied. These considerations result from analysis of the crystal structures of α- and γ-iPP and do not necessarily imply a definite mechanism of crystal growth, even if, in the case of γ-iPP, it is hard to envisage something different from chain deposition on 001 faces (cell III indexing).

5. Concluding Remarks

The usefulness of the present model in explaining the peculiarities of crystalline iPP may be illustrated with reference to the unusual angle of 40° that chain axes make with the normal to the lamellar surface in the γ phase.[7] This conclusion, reached by Lotz, Graff, and Wittmann on the basis of electron diffraction data referred to cell I, is still valid in the new cell III with the difference that, with the new indexing, the axis orthogonal to the lamellar surface is now *b* and it makes an angle of 40° with the axes of both crossing chains. While the value of 40° is highly unusual if referred to a set of parallel chains, it is much more understandable in this situation where, as is shown in Figure 6, a balanced tilting of nonparallel chains occurs.

Note that the resulting crystal architecture is still compatible with lamellar morphology. However, because of the different chain axis orientations with respect to the lamellar surface, the α and the γ polymorphs are unlikely to coexist within the same lamella. Accordingly, the two crystalline phases have been reported to coexist only within needlelike crystals of very low molecular weight iPP.[1] Furthermore, the dramatic structural differences between the α and γ crystals indicate that any hypothesis concerning a solid–solid γ-iPP to α-iPP transition[37,38] is extremely unlikely, and critical reexamination of the evidence suggesting the occurrence of such a process appears to be necessary.

In Figure 7 the geometry of α–γ branching[7] according to the new γ-iPP crystal architecture is shown. The angle of 40° between the daughter and the parent lamella can be explained by a mechanism in essence identical with the one proposed for α–α branching, i.e., epitaxial deposition of chains with an 80° tilt with respect to those in the

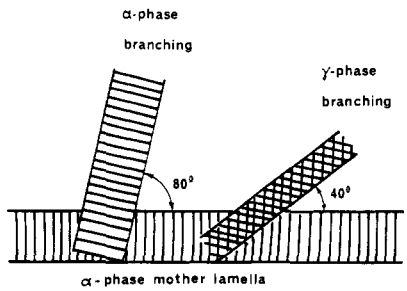

Figure 7. Schematic representation of α and γ branching occurring in iPP. The view and the symbolism are the same as in Figure 6 and are adapted from similar schemes devised by Lotz et al.[7] Note that in both α and γ branching crystals a chain axis orientation at 80° with one of the parent lamella is observed; in γ branches the other helical axis orientation is parallel to one of the α mother lamella. This scheme suggests the possibility of a common mechanism for α–α and α–γ branching.

mother lamella. According to previously suggested γ-iPP crystal models,[1,13] the observed branching morphology[7] required chains in the two crystals to be parallel, making it somewhat hard to explain why branching rather than further α-crystal growth would occur. It should be mentioned that the absence of branching phenomena in γ-iPP is also satisfactorily accounted for, as the process leading to branching in α-iPP involves a normal growth in γ-iPP.

With respect to the suggested reduced importance of chain folding in the γ polymorph,[6,7] we can only observe that, while our structure does not rule out the possibility of folds, a model substantially different from other polymer crystals is envisaged, which might well restrict chain folding.

The fundamental issue of the driving force leading to this new crystalline architecture rather than to the α modification remains open. The complexity of the γ-iPP crystal structure and the fact that it is favored by slow crystallization at comparatively high temperatures suggest that thermodynamic effects might have a prevailing role in γ crystallization. Further clarification of this question is likely to result from packing energy analysis comparing the internal energy of the α and the γ polymorphs. However, the question is further complicated because preferential γ crystallization occurs only in the presence of disturbing influences that have been mentioned in the Introduction. While it appears intuitively acceptable that the complex γ architecture is favored by low molecular weights, effects such as the possibly greater ability to include molecular defects in the crystal, fold surface influences, or more favorable free energy versus pressure dependence in the γ as compared to the α phase might also involve entropic factors. Certainly this behavior cannot be rationalized simply by comparing the α and the γ structures of isotactic polypropylene. Rather, these crystal structures are the starting point for an examination of the perturbative effects leading to γ crystallization.

Acknowledgment. This research has been partly supported by C.N.R., Italy (progetto strategico "Metodologie cristallografiche avanzate"), and M.P.I., Italy.

References and Notes

(1) Morrow, D. R.; Newman, B. A. *J. Appl. Phys.* **1968**, *39*, 4944.
(2) Sauer, J. A.; Pae, K. D. *J. Appl. Phys.* **1968**, *39*, 4959.
(3) Turner-Jones, A. *Polymer* **1971**, *12*, 487.
(4) Zambelli, A., private communication. Chien, J. C. W., private communication.
(5) Kaminsky, W.; Kulper, K.; Britzinger, H. H.; Wild, F. R. W. P. *Angew. Chem., Int. Ed. Engl.* **1985**, *24*, 507.
(6) Morrow, D. R. *J. Macromol. Sci.* **1969**, *B3*, 53.
(7) Lotz, B.; Graff, S.; Wittmann, J. C. *J. Polym. Sci., Polym. Phys. Ed.* **1986**, *24*, 2017.
(8) Petraccone, V.; Pirozzi, B.; Meille, S. V. *Polymer* **1986**, *27*, 1665.
(9) Padden, F. J., Jr.; Keith, H. D. *J. Appl. Phys.* **1973**, *44*, 1217.
(10) Khoury, F. *J. Res. Natl. Bur. Stand.* **1966**, *70A*, 29.
(11) Binsbergen, F. L.; De Lange, B. G. M. *Polymer* **1968**, *9*, 23.
(12) Corradini, P.; Petraccone, V.; Pirozzi, B. *Eur. Polym. J.* **1983**, *19*, 299.
(13) Turner-Jones, A.; Aizlewood, J. M.; Beckett, D. R. *Makromol. Chem.* **1964**, *75*, 134.
(14) Immirzi, A. *Acta Crystallogr., Sect. B* **1980**, *B36*, 2378.
(15) Brückner, S. *Chim. Ind. (Milan)* **1988**, *70*, 48.
(16) Rietveld, H. M. *J. Appl. Crystallogr.* **1969**, *2*, 65.
(17) Brückner, S.; Meille, S. V. *Nature* **1989**, *340*, 455.
(18) Grassi, A.; Zambelli, A.; Resconi, L.; Albizzati, E.; Mazzocchi, R. *Macromolecules* **1988**, *21*, 617.
(19) Natta, G.; Corradini, P. *Nuovo Cim. Suppl.* **1960**, *15*, 40.
(20) Mencik, Z. *J. Macromol. Sci.* **1972**, *B6*, 101.
(21) Lotz, B.; Wittmann, J. C. *J. Polym. Sci., Polym. Phys. Ed.* **1986**, *24*, 1541.
(22) Allegra, G.; Bassi, I. W.; Meille, S. V. *Acta Crystallogr., Sect. A* **1978**, *A34*, 652.
(23) Perego, G.; Cesari, M.; Allegra, G. *J. Appl. Crystallogr.* **1984**, *17*, 403.
(24) Albinati, A.; Willis, B. T. M. *J. Appl. Crystallogr.* **1982**, *15*, 361.
(25) Brückner, S.; Di Silvestro, G.; Porzio, W. *Macromolecules* **1986**, *19*, 235.
(26) Brückner, S.; Luzzati, S.; Porzio, W.; Sozzani, P. *Macromolecules* **1987**, *20*, 585.
(27) Brückner, S.; Luzzati, S. *Eur. Polym. J.* **1987**, *23*, 217.
(28) Brückner, S.; Porzio, W. *Makromol. Chem.* **1988**, *189*, 961.
(29) Brückner, S.; Meille, S. V.; Porzio, W. *Polymer* **1988**, *29*, 1586.
(30) Brückner, S.; Meille, S. V.; Malpezzi, L.; Cesaro, A.; Navarini, L.; Tombolini, R. *Macromolecules* **1988**, *21*, 967.
(31) Hay, J. N.; Kemmish, D. J.; Langford, J. I.; Rae, A. I. M. *Polym. Commun.* **1984**, *25*, 175.
(32) Hay, J. N.; Kemmish, D. J.; Langford, J. I.; Rae, A. I. M. *Polym. Commun.* **1985**, *26*, 283.
(33) Langford, J. I. *Prog. Cryst. Growth Charact.* **1987**, *14*, 185.
(34) *International Tables for X-Ray Crystallography*; Kynoch Press: Birmingham, England, 1969; Vol. I.
(35) Marega, A.; Marega, C.; Zannetti, R.; Paganetto, G.; Canossa, E.; Coletta, F.; Gottardi, F. *Makromol. Chem.* **1989**, *190*, 2805.
(36) Ferro, D. R.; Brückner, S.; Meille, S. V., manuscript in preparation.
(37) Kardos, J. L.; Christiansen, A. W.; Baer, E. *J. Polym. Sci., Part A-2* **1966**, *4*, 777.
(38) Newman, B. A.; Song, S. *J. Polym. Sci., Part A-2* **1971**, *9*, 181.
(39) Eufri, D.; Sironi, A. *J. Mol. Graphics* **1989**, *7*, 165.

Registry No. iPP, 25085-53-4.